



Characterization and calibration of MFM tip. Quantitative measurements in Magnetic Force Microscopy.

Theory basics

Since the majority of all Scanning Probe Microscopy techniques is based on the force or force derivatives detection, the starting relation is:

$$\mathbf{F} = \nabla E_{tip-sample}$$

where $E_{tip-sample}$ is an energy of tip-sample interaction.

Particularly for Magnetic Force Microscopy $E_{tip-sample}$ can be expressed in terms of a convolution of a tip magnetization \mathbf{M}_{tip} and a stray field from the sample \mathbf{H}_{sample} or, vice versa, as a convolution of the tip stray field \mathbf{H}_{tip} and the sample magnetization \mathbf{M}_{sample} :

$$E_{tip-sample} \sim \int_{tip} \mathbf{M}_{tip} \mathbf{H}_{sample}$$

$$E_{tip-sample} \sim \int_{sample} \mathbf{M}_{sample} \mathbf{H}_{tip}$$

where integration is performed over the whole magnetic volume of the tip (first relation) or the sample (the second one). In case of no perturbation between the tip and the sample both approaches should give equal results.

Therefore, generally speaking, having measured forces (or their derivatives) acting between a tip and a sample, it is theoretically possible to restore tip magnetization distribution \mathbf{M}_{tip} if stray field from the sample \mathbf{H}_{sample} is known in detail. And then, using so calibrated tip with known \mathbf{M}_{tip} one can extract stray field distribution from unknown sample using MFM scanning. Vice versa, upon some model assumptions on distribution of the stray field from MFM tip \mathbf{H}_{tip} and having assessed this value numerically, one can restore magnetisation distribution \mathbf{M}_{sample} within unknown sample. At the same time, care should be taken in interpreting a stray fields out of the media emanating them because exactly the same outer distribution of magnetic field can be generated with different bulk conditions [1174].

In most cases, and for MFM in particular, tip-sample interaction is substantially one-dimensional and consideration of only z-component of force derivative F'_z gives satisfactory numerical estimations:

$$\frac{\partial}{\partial z} F_z = \frac{\partial^2}{\partial z^2} E_{tip-sample}$$

By now phase shift detection scheme is most widespread for force gradient mapping in MFM because phase shift is proportional to the force derivative \mathbf{F}' :

$$\Delta\varphi = -\frac{Q}{k} \frac{\partial}{\partial z} F_z = -\frac{Q}{k} \frac{\partial^2}{\partial z^2} E_{tip-sample}$$

Besides one-dimensional approximation, a number of another simplifications are made due to complexity of the problem of magnetic interactions.

First, one can only guess on the real distribution of magnetisation \mathbf{M}_{tip} in the MFM tip. Therefore, some simplified models has been proposed to replace real tip with an appropriate approximation.

There are two most widespread approaches developed to date: point probe model [2649] and extended (magnetic) charge model including a number of their implementations.

Point probe model assumes that magnetic tip can be replaced with a single magnetic pole of monopole q or dipole \mathbf{m} nature, both being constant scalar and vector respectively (Fig. 1a).

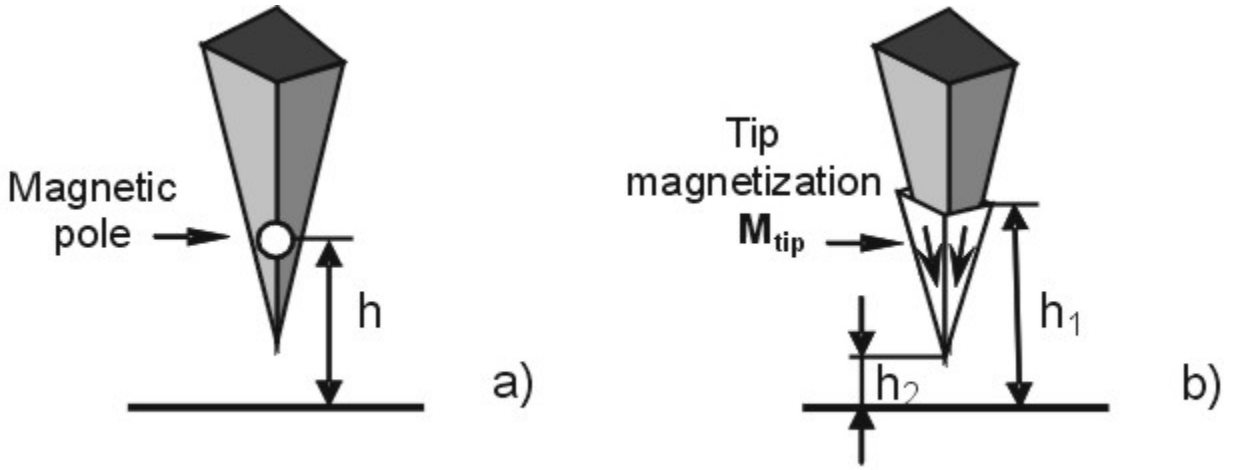


Fig. 1. The most widespread models of MFM tip. a) Point probe model. MFM tip is approximated by a single point pole of monopole q or dipole \mathbf{m} nature. b) Extended charge model. One of the model implementation is shown. MFM tip is approximated by pyramid with different magnetization vectors on different facets. Active imaging volume is depicted in white. See also Fig. 3.

Expression for monopole approximation can be written as:

$$\mathbf{F}_q = \nabla \int_{tip} \mathbf{M}_{tip} \mathbf{H}_{sample} dV_{tip} \rightarrow -q \cdot \mathbf{H}_{sample}$$

and for dipole approximation as:

$$\mathbf{F}_m = \nabla \int_{tip} \mathbf{M}_{tip} \mathbf{H}_{sample} dV_{tip} \rightarrow (\mathbf{m} \cdot \nabla) \mathbf{H}_{sample}$$

$$\mathbf{m} = \mathbf{M}_{eff} V_{eff}$$

where \mathbf{M}_{eff} is effective uniform tip magnetization and V_{eff} is effective imaging volume of the tip.

Combining both contributions the resulting force in one-dimensional case can be expressed as:

$$F_z = -qH_z + m_x \frac{\partial H_x}{\partial z} + m_y \frac{\partial H_y}{\partial z} + m_z \frac{\partial H_z}{\partial z}$$

and force derivative as

$$\frac{\partial F}{\partial z} = -q \frac{\partial H_z}{\partial z} + m_x \frac{\partial^2 H_x}{\partial z^2} + m_y \frac{\partial^2 H_y}{\partial z^2} + m_z \frac{\partial^2 H_z}{\partial z^2}$$

As a matter of fact, point pole approximation is rather rough due to above simplifications, and fails to explain entire stray field from the tip [2604]. The advantage is that the field calculation is simple and application to the theory of MFM is straightforward. This approach is continuously being applied by many researchers.

Extended charge model looks much more realistic assuming that magnetic charges in the tip volume are nonpoint like (Fig. 1b). Unfortunately, implementations of this model are more complicated. Working in Fourier domain helps to simplify calculations in this case.

Both models become inaccurate if the samples with characteristic dimensions of magnetic features different from those used for calibration are investigated. By now neither model is able to guarantee "absolute" calibration of the given tip. Thus, recalibration for various samples is necessary.

Limitations of current magnetic force imaging techniques give rise to refinement of existent theoretical backgrounds and development of novel experimental approaches such as that described by Schaffer et al. [2597]. The process to find out reliable and universal quantification in MFM steadily goes on.

One should also take into consideration, that measured MFM signal is a convolution of so-called instrumental response function and pure MFM signal. So, to extract pure MFM signal specific deconvolution procedures should be performed. This effect is as much as smaller are the magnetic features on the sample surface.

Experimental techniques

A number of approaches have been proposed to acquire both qualitative and quantitative description of magnetic tips in order to make MFM imaging quantitative. These approaches can be divided into two main groups: techniques based on MFM scanning over current carrying structures formed on a calibration sample surface and the others which use another principles involving MFM for successive correction of initial approximations or do not use MFM at all.

Let us begin from the second group. This group comprises Resonant Torque Magnetometry (RTM) [2633, 2621], Lorentz electron tomography [2603], electron holography [2664] and some other methods.

These methods help understanding peculiarities of magnetic field distribution in the nearest vicinity of the magnetic tip and are to be considered as independent ways to develop reliable and simple MFM-like method of tip characterization/calibration.

Resonant Torque Magnetometry allows a hysteresis loop to be obtained by applying a local field to the tip, either along the tip axis or normally to it, and measuring torque response of the tip [2621]. A sensitivity of better than 10^{-12} emu (10^{-15} A·m²) has been reported by Heiydon et. al [2633]. Measurements were performed in-situ that is of great importance especially when images are made in the presence of bias fields. At the same time this technique is rather exotic and cannot be implemented in common laboratories. RTM also impose some limitations to the measuring conditions.

Lorentz electron tomography used by McVitie et al. [2603] registers deflection of accelerated electron beam influenced by magnetic field in the nearest vicinity of MFM tip (Fig. 2).

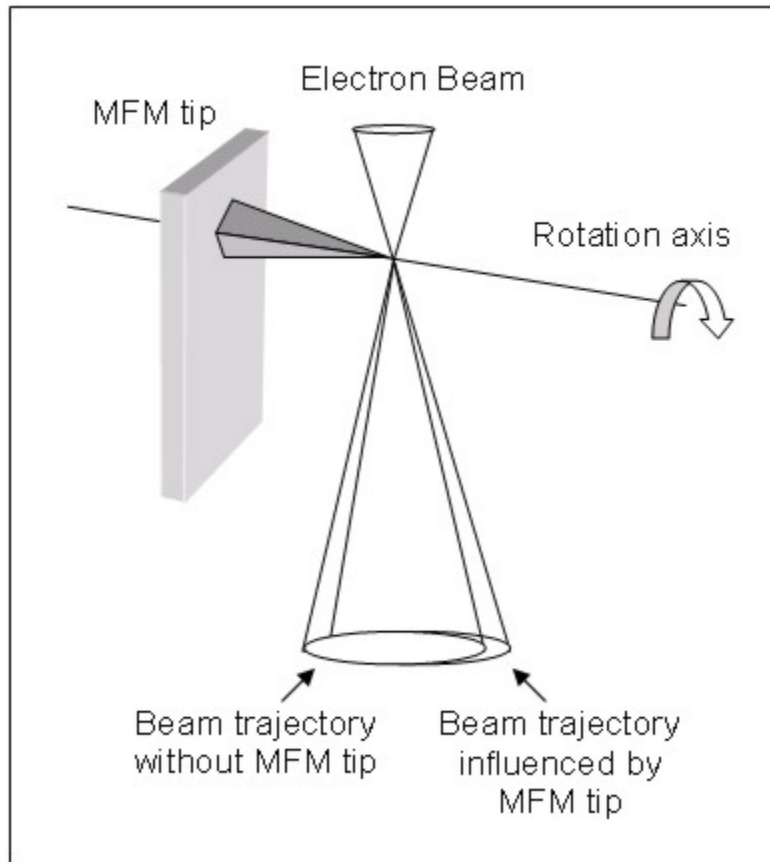


Fig. 2. Schematic of differential phase contrast imaging technique of Lorentz microscopy applied to a MFM tip (McVitie et al. [2603]). This imaging mode is implemented on a scanning transmission electron microscope.

This technique gives the real, but integral field distribution near the tip apex not distorted by any external fields. The data obtained easily reveal anisotropy of the field around the axis of the tip due to its nonideal pyramidal form. Small tilt over the measured surface as well as some unwanted effects ([2663]) also contribute to the final result. Then, specific tomographic reconstruction is implemented to restore the real field distribution. The authors compared data obtained by electron tomography with the results of calculations according to most common approximations of MFM tip magnetic state such as point pole and extended charge models. It was found that the field from MFM tip has contributions which are point like and nonpoint like. While the central part of the field can be well represented by a point or localized charge, the modeling of extended tails of the field implies nonlocal magnetic charge distribution. The profile of magnetic field using extended charge model (Fig. 3) can be ideally fitted by means of fitting parameters. There are, though, some difficulties in interpretation of thus obtained results.

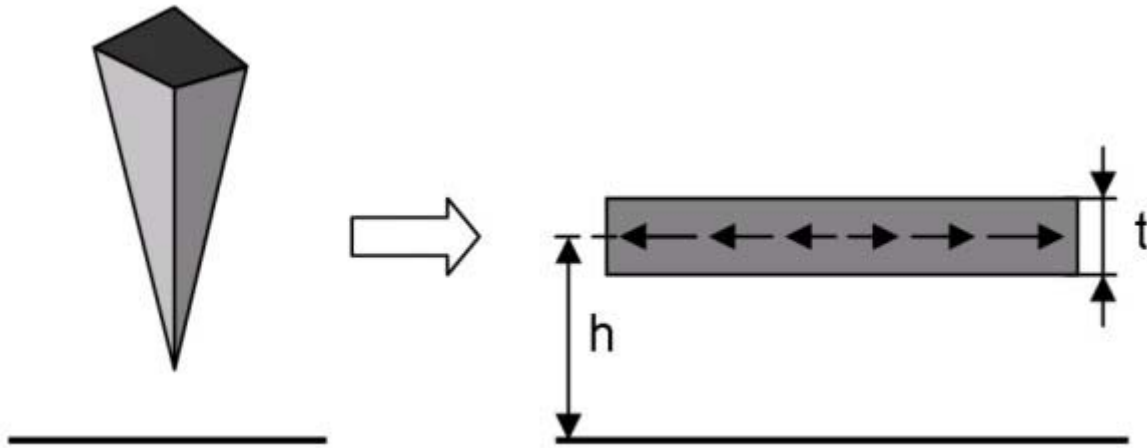


Fig. 3. Representation of MFM tip by magnetic layer of thickness t with predefined magnetization distribution according to extended charge model used by McVitie et al. [2603] for Fourier space calculations.

Another technique involving multiple MFM sessions and Fourier transforms is developed by Hug, van Schendel et al. [2632, 2604]. It is a sophisticated iterative procedure for MFM tip calibration using transfer-function approach. The sample under scanning is specialty sandwich-like Cu/Ni/Cu structure with strong perpendicular magnetization. Authors came to conclusion that the point monopole and dipole models of the MFM tip are not suitable to describe the tip calibrations found in the experiment. And in spite of the fact that a reasonable agreement between the simulation and the measurement is obtained with a monopole model with additional tip-sample distance, it is not recommended to use a point pole model for the evaluation of MFM data acquired on a sample with domains with a different size than those of the sample used for calibration. Even using extended charge model one should recalibrate the tip to investigate samples with magnetic feature sizes different from used for calibration. The authors found point pole probe approach inadequate when interpreting submicron magnetic features which are comparable to the tip size, though this approach may be still applicable for the structures with relatively large features and large lift heights. The maximum magnetic flux density at the tip end was estimated about 0,01 Tesla for about 10 nm Fe layer covered with about 15 nm Au coatings. The sensitivity is found to be in the microtesla range for stray field variations on the order of 100 nm.

By common practice, determination of a sample stray field using calibrated MFM tip of given magnetization \mathbf{M}_{tip} is the most often task investigators have to encounter. This task is successfully solved using MFM tips calibrated by means of the first group techniques. It is obvious, that only current carrying metal stripes are able to produce well-controllable and regular magnetic field with predefined distribution $\mathbf{H}_{\text{sample}}$ to restore tip magnetization \mathbf{M}_{tip} . Due to micron and submicron scales these stripes are manufactured by electron beam lithography and may differ in geometry. The following types of strip lines are reported so far: one straight strip line [2582, 2619]; two or more straight strip lines [2599, 2600, 2631, 2634, 2635, 2639], current rings [2612, 2636, 2637].

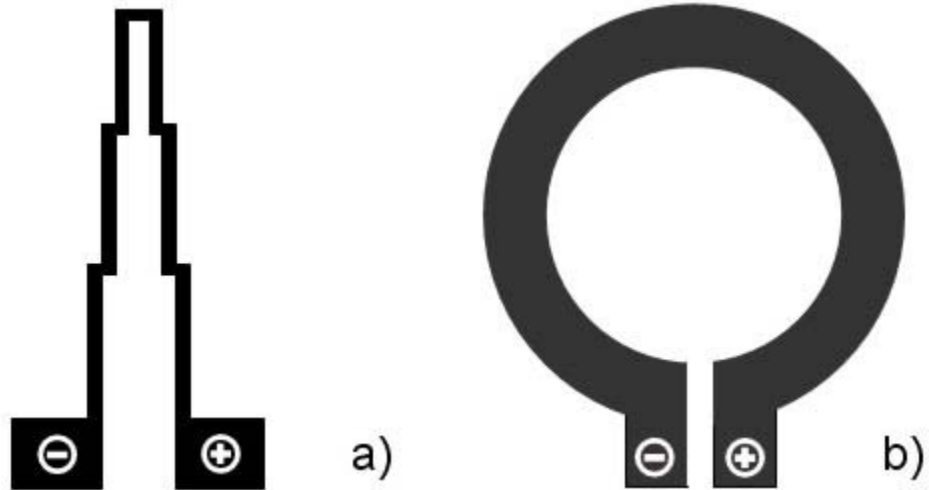


Fig. 4. Typical current strip line configurations for generating of well-defined magnetic field. a) Two parallel strip lines with regions of various distance between lines (Goddenhenrich et al. [2631]). b) Current ring (Kong and Chou [2636, 2637], Lohau et al. [2612]).

The first attempt to compare calculated and measured magnetic forces acting between a tip and a sample using current carrying strip lines was undertaken by Goddenhenrich et al. [2631] in early 90-s (Fig. 4a)). The authors have got satisfactory qualitative agreement of calculated and measured curves. To get semiquantitative results convolution effects due to finite tip size should be also taken into consideration.

The distribution of magnetic field gradient for a couple of straight lines is shown in Fig. 5. Simple and comprehensible animations help to understand how magnetic field and its gradient are distributed over the current carrying lines.

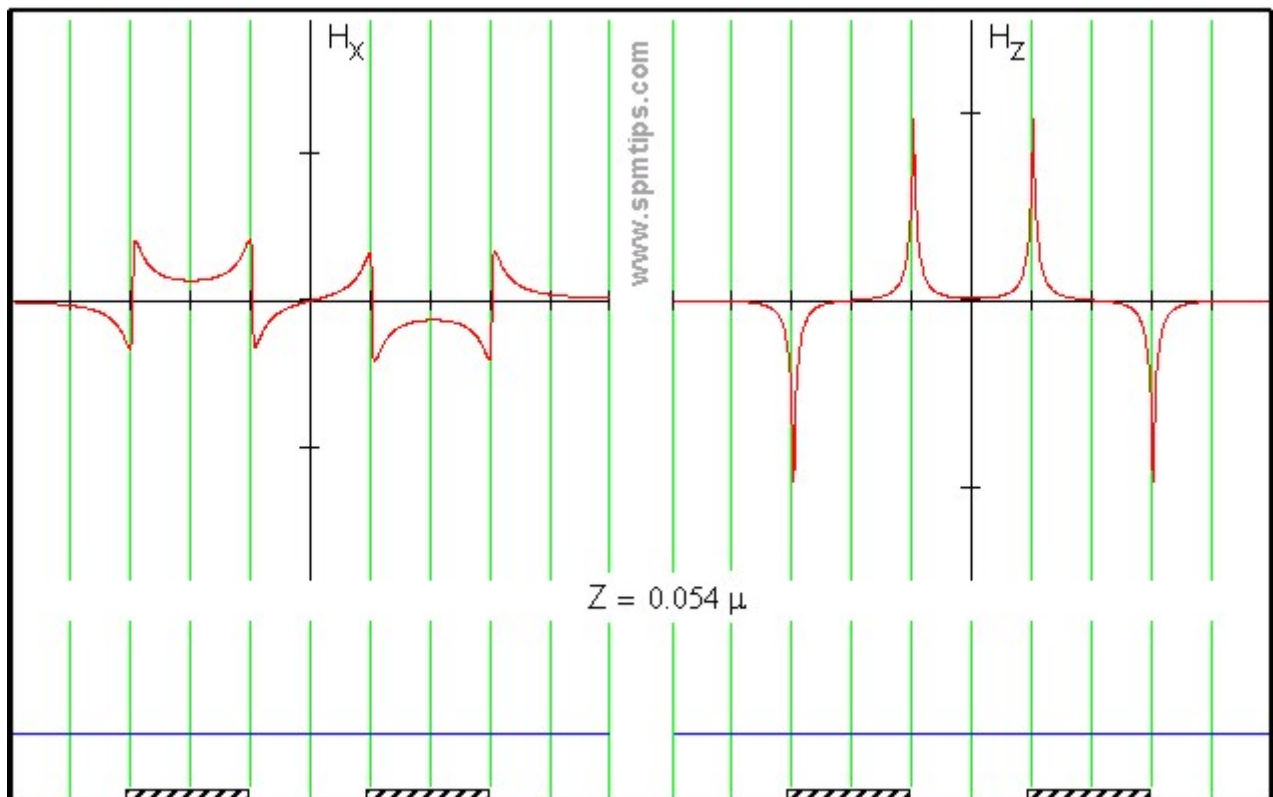


Fig. 5. Distribution of horizontal H_x and vertical H_y components of magnetic field gradient over two current carrying strip lines of opposite polarity upon height Z in microns. The lines go in parallel to each other and their cross sections are only shown. Both components are plotted separately for convenience. Click on the picture to download the full animation (80 Kb in a self-extracting archive).

One can see that distribution of H_x component is symmetrical relative to the strip line profile, and that of H_z is antisymmetrical. After viewing the full animation it is obvious that the distribution of H_x component changes drastically upon vertical distance Z as opposed to H_y which changes in amplitude only.

Yongsunthon et al. [2599] consider MFM as a useful method for studying electromigration in metals which is of vital importance due to continuous shrinkage of integrated circuit dimensions. Proposed calibration structure comprises three metal strip lines (Fig. 6), of which the left is null-potential grounded line connected to the tip, the central line includes small slit in the central part thus modeling defect, and the right line is reference one of well defined geometry.

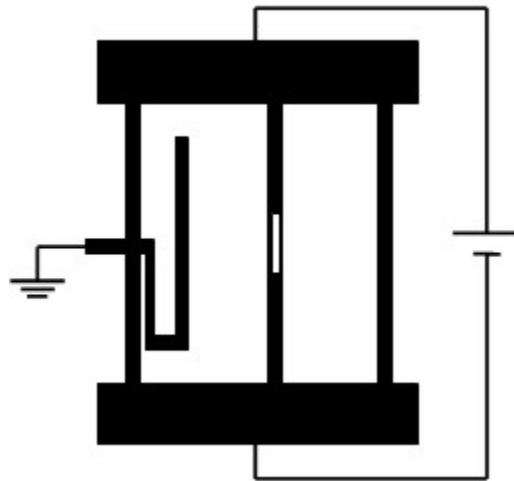


Fig. 6. Current strip line configuration used for in situ calibration of MFM tip by Yongsunthon et al. [2599].

Null-potential line guarantees the absence of electrostatic component among various tip-sample interactions. It serves to indicate that no phase shift is present when the tip is scanning above this area. The reference structure is used to normalize the signal magnitude from the test structure. Also it is intended to determine iteratively so-called instrumental response function which enables deconvolution of measured MFM signal in order to extract pure MFM response. Using dipole moment approximation in accordance with point probe model, relative quantification of the MFM signal amplitude to within 10% can be achieved and absolute current variations can be detected to at least 10%.

Successful application of MFM imaging to map quantitatively current densities around various defects in metal conductors is reported in the latest works of Yongsunthon et al. [2639] and Rose et al. [2600].

Results presented lately by Kebe and Carl [2634] reflect progress made for more than a decade in MFM tip calibration using current carrying structures. Beginning from current rings in early works, the authors consider various parallel wire configurations in this ample paper. Analysis is again conducted using point probe model for approximation of MFM tip. Having studied many configurations of current carrying lines authors related point probe parameters to the dimensions of parallel wires and to characteristic decay length of the z -component of the magnetic field produced with them. This allowed to determine the effective volume V_{eff} of the real magnetic tip relevant in MFM imaging. The authors proposed experimental technique which allows quantitative measurement of the magnetization of nanoscale ferromagnetic elements with an in-plane magnetization by calibrated MFM tip.

Kong and Chou have pioneered in using current rings for MFM tip calibration purposes [2636, 2637]. Using monopole and dipole approximations within a point pole model the authors found that at different lift heights both moments contribute unequally, which gave rise to the final conclusion that only the dipole moment is relevant for imaging.

Lohau et al. [2612] thoroughly studied applicability of point pole model to the quantitative determination of magnetic state of the tip using current rings of various radii. It was found that MFM images can only be analyzed unambiguously within the point pole approximation when using either the dipole or the monopole contribution taking into account heights of the point pole above the sample surface which are different in each case. Both point probe approaches was found to give identical results independent of the lift height used and it is therefore not necessary to consider a mixture of both contributions.

A number of papers describe changes in magnetization of MFM tips imposed by external magnetic fields. Use of current carrying structures becomes here the only way to determine tip magnetic state because any other magnetic sample is critically affected under strong fields applied, whereas the stray field from such current carrying structures is kept unchanged. Knowing magnetization reversal of the tip one can study magnetization reversal of magnetic samples.

Typical hysteresis loops for tips of various shape and covered with various coatings are presented in Fig. 7.

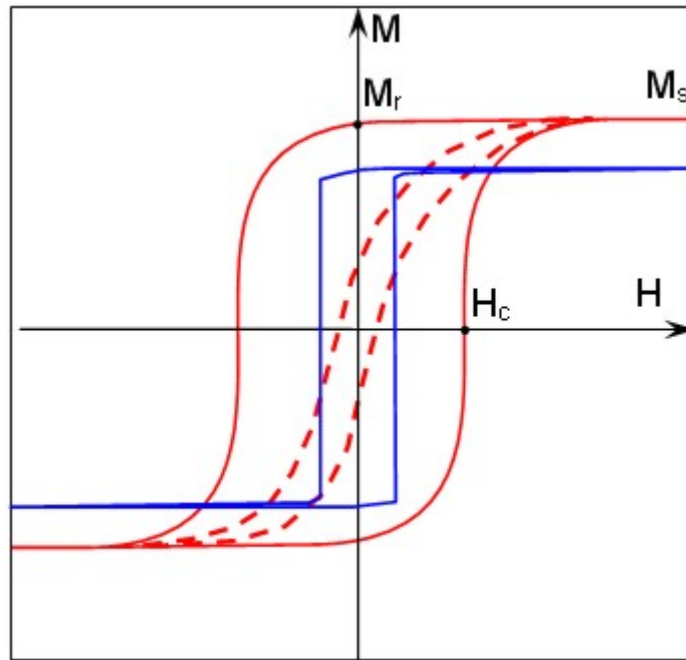


Fig. 7. Typical hysteresis loops obtained for various metal coatings of MFM tips. High coercivity coating has a broad hysteresis loop (solid red line). Low coercivity coating has a narrow loop (dashed red line). Blue line reflects behaviour of coating deposited on narrow and long tip. This coating switches as a single domain particle under varying external field and features almost square hysteresis loop. H_c , M_r and M_s stand for coercivity, remanent magnetization and saturation magnetization respectively.

In general, magnetic coatings can be divided into two categories: made of high coercivity (CoCr, CoCrPt etc.) and low coercivity (FeNi, FeCoNi etc.) materials. There were also reports about superparamagnetic [2730, 2567], paramagnetic [2705], antiferromagnetic [2711] or multilayer [2691] MFM tips. The proper choice depends upon the purposes of a given study. It is found experimentally that typical coercivity of CoCr tips is between 300-400 Oe, and for low-coercivity tips H_c amounts to 1-5 Oe or less.

One should remember, that high coercivity tips may influence the sample magnetic structure and vice versa. Such perturbation leads to displacement of domain walls [2615, 2748, 2749], irreproducibility of successively taken images [1111, 1122], and another unwanted effects. As for imaging in applied external magnetic fields, it is desirable to use a tip either having coercivity far beyond that of the sample (so that the applied field does not affect the tip), or far below it (so that the

tip moment is always aligned with applied field) [2582]. Tapping the sample with the MFM tip during topography acquisition in interleave or "liftmode" may significantly perturb magnetization distribution in the sample or in the tip. Therefore, if sample topography is sufficiently smooth, noncontact imaging at fixed height is preferable instead of two-pass technique such as liftmode.

The more aspect ratio of the tip, the more uniform and predictable is magnetization distribution in the volume of magnetic coating. The utmost case is narrow needle shaped tip proved to be monodomain, so hysteretic loop of such a tip is of almost square shape (so-called coefficient of squareness is close to 1.00).

Babcock et al. [2582] systematically studied the magnetic states of a set of MFM probes as a function of uniform external magnetic field using single current strip line. In order to avoid influence of electrostatic forces entire structure was covered by thin insulating and metal coatings, the latter being grounded during MFM measurements. It was shown that there are two different response characteristics for lateral and vertical components of remanent magnetization in the phase images. Vertical component gives antisymmetric response and the lateral - symmetric one. Such an effect is easily seen from the field gradient profiles, plotted in Fig. 5. The authors show that after magnetizing even in a strong lateral fields remanent state is apparently far from horizontal orientation but tilted 30-40° relative to the plane of the sample.

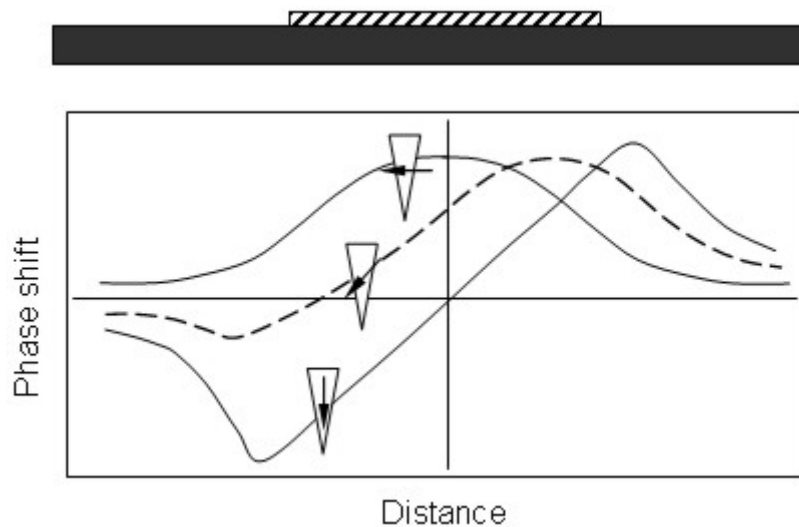


Fig. 8. Responses of the MFM tip scanning the single strip line (shown above) under various orientations of external field. (after Babcock et al. [2582])

Carl et al. [2569] describes an experimental technique to determine magnetization reversal and coercivity of MFM tips using current carrying metal ring. Measurements were conducted in the central part of substantially large ($\varnothing=2400$ nm) ring. Such a big size guarantees that mainly vertical H_z component is present in the central part of the ring and there are no electrostatic forces present in this area, so shielding metal coating was not exploited. Coercivity H_c , remanent magnetization M_r , and saturation magnetization M_s of the tips from corresponding hysteresis loops were obtained changing external field from H_z to $-H_z$.

It was found that properties of theoretically identical tips from various wafers differ widely, sometimes by factor of 2. This discrepancy can only be attributed to unequal manufacturing conditions rather than to other reasons. Typical coercivity for CoCr coated tips were found to be within 270-360 Oe and remanent magnetization $M_r=869-1336$ emu/cc. For comparison the same characteristics were gathered by Superconducting Quantum Interference Magnetometry (SQUID Magnetometry). Values obtained by SQUID measurements differed from that of MFM widely. For example, $H_{c,SQUID}/H_{c,MFM}$ relation lie within 0,9...2,2 range. It is only MFM that allow estimation of the volume of the tip relevant for image formation. Therefore, the choice in favour of MFM rather than SQUID magnetometry is preferable to assess most common magnetic properties of the probing tip.

Using so calibrated tip Lohau, Carl et al. [2602] determined quantitatively the hysteresis loop of a single magnetic dot of 230 nm in diameter taking into account the correction for the tip reversal properties. The technique described in the paper allows one to measure precisely the coercivity of a given sample $H_{c, \text{sample}}$ even if it is comparable with the coercivity of the tip itself. Furthermore, the shape of the hysteresis loop of small magnetic elements may be obtained with sufficient accuracy in order to be able to differentiate, e.g., between different reversal modes of magnetic elements.

In conclusion, some general regularities will be given concerning resolution and sensitivity in MFM measurements.

Probe sensitivity over the current strip line can be estimated in terms of minimal magnetic moment within point dipole approximation:

$$m \approx \frac{2k\Delta f_0}{f_0} \left(\frac{\partial^2 H_z}{\partial z^2} \right)^{-1}$$

where f_0 - resonant frequency shift. For example, in case of most commonly used CoCr coatings m_z of $\sim 6 \cdot 10^{-12}$ emu has been reported [2582].

MFM resolution and magnitude of the contrast observed in MFM depend upon the geometry and size of the magnetic material which interacts with the sample stray field. Such working part is also called "active volume" of the MFM tip (depicted in white in Fig 1b). Both resolution and contrast for "magnetically hard" MFM probes increase as the final portion of the tip goes long and narrow having flat end [2645]. Such tips are manufactured using Electron Beam Deposition [2643, 2728] or Focused Ion Beam [2647, 2691] techniques. At the same time one should remember, that such tips are easily worn during tapping while acquiring topography by means of widely used two-pass technique. So, noncontact mode is preferable if no great topography variations are present on the sample surface.

Horizontal and vertical resolution of MFM imaging differs greatly. Commercial tips are intended mainly for sensing of vertical field component whereas in-plane components are often out of their capabilities. To make tip sensitive to lateral forces, one should manage to make the very end of the tip magnetized horizontally. Simple applying of external magnetic field in horizontal direction will give a little success. The remedy could be making nanoscopic pinhole in the very apex of the magnetic tip as offered by Folks et al. [2610]. This lead to occurrence of very small region with sufficiently strong horizontal magnetic moment. Another three- step way to extract information about distribution of lateral magnetic moments from MFM scans is described by Zhao et al. [2648].

Abelmann et al. [1108] reported results of a great study devoted to comparing the resolution of MFM from various manufacturers using special reference samples consisting of CoNi/Pt magneto-optic multilayers with different thicknesses. It was found that resolution does not vary considerably between the different instruments and lies within 30-100 nm range. Theoretical analysis shows that maximum resolution is governed by the distance between magnetic charges in the sample and in the tip which is quite different from the physical tip-sample separation. The lower the separation the higher resolution. Though, reduction of physical tip-sample separation leads to a plenty of smaller details or even artefacts of nonmagnetic origin. Therefore, reduction of magnetic rather than physical distance between interacting charges becomes a matter of art.

Dependence of MFM data on the tip magnetization orientation has been studied by Litvinov and Khizroev [2709], who manufactured the finest cylindrical MFM tip of 50 nm in diameter and 10 nm in height which is one of the best ever reported physical implementation of the "dipole moment" MFM probe. By controlling the preferred orientation of the magnetization, it is possible to define directional sensitivity. The preferred orientation is controlled either by choosing a proper magnetic material with preferred crystalline anisotropy or by applying a sufficiently strong external magnetic field.

Complete list of references to the articles devoted to MFM-related problems is placed in the [Reference Collections](#) section of our [Library](#).

Please, send all comments and suggestions concerning these pages to Library@mikromasch.com

ID	Reference list (newly come references are marked red)
2649	The point dipole approximation in magnetic force microscopy U. Hartmann <i>Phys. Lett. A</i> , 137 (1989) 9, 475-478
2631	Probe calibration in magnetic force microscopy T. Goddenhenrich, H. Lemke, M. Muck, U. Hartmann, and C. Heiden <i>Appl. Phys. Lett.</i> , 57 (1990) 24, 2612-2614
1185	The influence of experimental parameters on contrast formation in magnetic force microscopy F. Kaisinger, H. Starke, G. Persch, U. Hartmann, F. Krause <i>Thin Solid Films</i> , 264 (1995) 2, 141-147
1185	The influence of experimental parameters on contrast formation in magnetic force microscopy F. Kaisinger, H. Starke, G. Persch, U. Hartmann, F. Krause <i>Thin Solid Films</i> , 264 (1995) 2, 141-147
1120	High-resolution magnetic imaging based on scanning probe techniques U. Hartmann <i>Journal of Magnetism and Magnetic Materials</i> , 157-158 (1996) 545-549
2664	Quantitative magnetometry using electron holography: field profiles near magnetic force microscope tips D.G. Streblechenko, M.R. Scheinfein, M. Mankos, K. Babcock <i>IEEE Trans. Magn.</i> , 32 (1996) 5, 4124-4129
1135	Magnetic force microscopy images of high-coercivity permanent magnets L. Folks, R. Street, R.C. Woodward, K. Babcock <i>Journal of Magnetism and Magnetic Materials</i> , 159 (1996) 1-2, 109-118
2582	Field-dependence of microscopic probes in magnetic force microscopy K. L. Babcock, V. B. Elings, J. Shi, D. D. Awschalom, and M. Dugas <i>Appl. Phys. Lett.</i> , 69 (1996) 705-707
1122	Interactions between soft magnetic samples and MFM tips S.L. Tomlinson, A.N. Farley, S.R. Hoon, M.S. Valera <i>Journal of Magnetism and Magnetic Materials</i> , 157-158 (1996) 557-558
2730	Superparamagnetic magnetic force microscopy tips P. F. Hopkins, J. Moreland, S. S. Malhotra, S. H. Liou <i>J. Appl. Phys.</i> , 79 (1996) 8, 6448-6450
2650	Quantitative Magnetic Field Measurements With The Magnetic Force Microscope Roger Proksch, George D. Skidmore, E. Dan Dahlberg, Sheryl Foss, J. J. Schmidt, and Chris Merton, Brian Walsh, Matt Dugas <i>Appl. Phys. Lett.</i> , 69 (1996) 17, 2599-2601
2728	Electron beam fabrication and characterization of high-resolution magnetic force microscopy tips M. Ruhrig, S. Porthun, and J. C. Lodder, S. McVitie, L. J. Heyderman, A. B. Johnston, and J. N. Chapman <i>J. Appl. Phys.</i> , 79 (1996) 6, 2913-2919
2745	Investigation of the domain contrast in magnetic force microscopy L. Belliard, A. Thiaville, S. Lemerle, A. Lagrange, J. Ferre, and J. Miltat <i>J. Appl. Phys.</i> , 81 (1997) 8, 3849-3851
2643	Improved spatial resolution in magnetic force microscopy G. D. Skidmore, E. D. Dahlberg <i>Appl. Phys. Lett.</i> , 71 (1997) 3293-3295
2733	A microfabricated tip for simultaneous acquisition of sample topography and high-frequency magnetic field V. Agrawal, P. Neuzil, and D. W. van der Weide

	<i>Appl. Phys. Lett.</i> , 71 (1997) 16, 2343-2345
2748	Magnetic dissipation force microscopy P. Grutter, Y. Liu, P. LeBlanc, and U. Durig <i>Appl. Phys. Lett.</i> , 71 (1997) 2, 279-281
2636	Quantification of magnetic force microscopy using a micronscale current ring Linshu Kong and Stephen Y. Chou <i>Appl. Phys. Lett.</i> , 70 (1997) 15, 2043-2045
2637	Study of magnetic properties of magnetic force microscopy probes using micronscale current rings Linshu Kong and Stephen Y. Chou <i>J. Appl. Phys.</i> , 81 (1997) 8, 5026-5028
2638	Micromagnetic model for magnetic force microscopy tips S. L. Tomlinson and A. N. Farley <i>J. Appl. Phys.</i> , 81 (1997) 8, 5029-5031
2633	Resonant torque magnetometry: a new in-situ technique for determining the magnetic properties of thin film MFM tips G.P. Heydon, A.N. Farley, E. Hoon, O. Valera, S.L. Tomlinson <i>IEEE Trans. Magn.</i> , 33 (1997) 5, 4059-4061
2568	Measurement of the stray field emanating from magnetic force microscope tips by Hall effect microsensors A. Thiaville, L. Belliard, D. Majer, E. Zeldov, J. Miltat <i>J. Appl. Phys.</i> , 82 (1997) 7, 3182-3191
2567	High resolution imaging of thin-film recording heads by superparamagnetic magnetic force microscopy tips S. H. Liou, S. S. Malhotra, John Moreland, P. F. Hopkins <i>Appl. Phys. Lett.</i> , 70 (1997) 1, 135-137
873	Magnetically refined tips for Scanning Force Microscopy R. Jumpertz, P. Leinenbach, A.W.A. van der Hart, J. Schelten <i>Microelectronic Engineering</i> , 35 (1997) 1-4, 325-328
2632	Quantitative magnetic force microscopy on perpendicularly magnetized samples Hans J. Hug, B. Stiefel, P. J. A. van Schendel, A. Moser, R. Hofer, S. Martin, H.-J. Guntherodt, S. Porthun, L. Abelmann, J. C. Lodder, G. Bochi, and R. C. O'Handley <i>J. Appl. Phys.</i> , 83 (1998) 11, 5609-5620
1174	On the determination of the internal magnetic structure by magnetic force microscopy B. Vellekoop, L. Abelmann, S. Porthun, C. Lodder <i>Journal of Magnetism and Magnetic Materials</i> , 190 (1998) 1-2, 148-151
1111	Development of high coercivity magnetic force microscopy tips S.H. Liou, Y.D. Yao <i>Journal of Magnetism and Magnetic Materials</i> , 190 (1998) 1-2, 130-134
1123	Interpretation of low-coercivity tip response in MFM imaging R. Street, D.L. Bradbury, L. Folks <i>Journal of Magnetism and Magnetic Materials</i> , 177-181 (1998) 980-981
1108	Comparing the resolution of magnetic force microscopes using the CAMST reference samples L. Abelmann, S. Porthun, M. Haast, C. Lodder, A. Moser, M.E. Best, P.J.A. van Schendel, B. Stiefel, H.J. Hug, G.P. Heydon, A. Farley, S.R. Hoon, Thomas Pfaffelhuber, R. Proksch, and K. Babcock <i>Journal of Magnetism and Magnetic Materials</i> , 190 (1998) 1-2, 135-147
2596	Optimization of lateral resolution in magnetic force microscopy S. Porthun, L. Abelmann, S.J.L. Vellekoop, J.C. Lodder, H.J. Hug <i>Applied Physics A: Materials Science & Processing</i> , 66 (1998) 7, S1185-S1189

1111	Development of high coercivity magnetic force microscopy tips S.H. Liou, Y.D. Yao <i>Journal of Magnetism and Magnetic Materials</i> , 190 (1998), 1-2, 130-134
1174	On the determination of the internal magnetic structure by magnetic force microscopy B. Vellekoop, L. Abelmann, S. Porthun, C. Lodder <i>Journal of Magnetism and Magnetic Materials</i> , 190 (1998), 1-2, 148-151
2749	Magnetic dissipation force microscopy studies of magnetic materials Y. Liu and P. Grutter <i>J. Appl. Phys.</i> , 83 (1998) 11, 7333-7338
2666	Comparing the resolution of magnetic force microscopes using the CAMST reference samples L. Abelmann, S. Porthun, M. Haast, C. Lodder, A. Moser, M. E. Best, P.J.A. van Schendel, B. Stiefe, H. J. Hug, G.P. Heydon, A. Farley, S.R. Hoon, Th. Pfaffelhuber, R. Proksch, K. Babcock <i>Journal of Magnetism and Magnetic Materials</i> , 190 (1998) 135-147
2619	Quantification of magnetic force microscopy images using combined electrostatic and magnetostatic imaging R. D. Gomez, A. O. Pak, A. J. Anderson, E. R. Burke, A. J. Leyendecker, and I. D. Mayergoyz <i>J. Appl. Phys.</i> , 83 (1998) 11, 6226-6228
1117	Fabrication and characterization of advanced probes for magnetic force microscopy U. Hartmann, J. Schelten, P. Leinenbach, U. Memmert <i>Applied Surface Science</i> , 144-145 (1999) 492-496
1147	Magnetic microscopies: the new additions - The Analysis of Magnetic Microstructures R. Proksch, E. Dan Dahlberg <i>Journal of Magnetism and Magnetic Materials</i> , 200 (1999) 1-3, 720-728
2611	Range of interactions: An experiment in atomic and magnetic force microscopy W. L. Murphy et al. <i>Am. J. Phys.</i> , 67 (1999) 905
2612	Quantitative determination of effective dipole and monopole moments of magnetic force microscopy tips J. Lohau, S. Kirsch, A. Carl, G. Dumpich, and E. F. Wassermann <i>J. Appl. Phys.</i> , 86 (1999) 3410-3417
1104	Calculation of playback signals from MFM images using transfer functions S.J.L. Vellekoop, J.J. Miles, J.C. Lodder, L. Abelmann, S. Porthun <i>Journal of Magnetism and Magnetic Materials</i> , 193 (1999) 1-3, 474-478
1116	Extracting media noise characteristics from MFM images T. Minvielle, S. Nair, P. Arnett <i>Journal of Magnetism and Magnetic Materials</i> , 193 (1999) 1-3, 479-483
1176	Preparation and characterisation of a new amorphous tip coating for application in magnetic force microscopy H.A. Davies, S. McVitie, M.R.J. Gibbs, R.P. Ferrier, W.M. Rainforth, J. Scott, G.P. Heydon, J.W. Tucker, J.E.L. Bishop <i>Journal of Magnetism and Magnetic Materials</i> , 205 (1999) 2-3, 131-135
1175	Potentiometric and magnetic force microscopy in multilayers D.B. Lambrick, M.A. Slade, H. Holloway, M.S. Valera, A.N. Farley, D.J. Kubinski, S.R. Hoon <i>Journal of Magnetism and Magnetic Materials</i> , 198-199 (1999) 95-97
2614	Observation of the effects of tip magnetization states on magnetic force microscopy images Paul Rice and Stephen E. Russek <i>J. Appl. Phys.</i> , 85 (1999) 8, 5163-5165
2615	Magnetic dissipation microscopy in ambient conditions Roger Proksch, Ken Babcock, and Jason Cleveland <i>Appl. Phys. Lett.</i> , 74 (1999) 419-421

1110	Description of magnetic force microscopy by three-dimensional tip Green's function for sample magnetic charges H. Saito, S. Ishio, J. Chen <i>Journal of Magnetism and Magnetic Materials</i> , 191 (1999) 1-2, 153-161
2621	Single layer and multilayer tip coatings in magnetic force microscopy S. M. Casey, D. G. Lord, P. J. Grundy, M. Slade, and D. Lambrick <i>J. Appl. Phys.</i> , 85 (1999) 8, 5166-5168
2605	Quantitative determination of the magnetization and stray field of a single domain Co/Pt dot with magnetic force microscopy J. Lohau, S. Kirsch, A. Carl, and E. F. Wassermann <i>Appl. Phys. Lett.</i> , 76 (2000) 3094-1096
2604	A method for the calibration of magnetic force microscopy tips P. J. A. van Schendel, H. J. Hug, B. Stiefel, S. Martin, and H.-J. Guntherodt <i>J. Appl. Phys.</i> , 88 (2000) 435-445
1126	Investigation of the response of a new amorphous ferromagnetic MFM tip coating with an established sample and a prototype device G.P. Heydon, W.M. Rainforth, M.R.J. Gibbs, H.A. Davies, J.E.L. Bishop, J.W. Tucker, S. Huo, G. Pan, D.J. Mapps, W.W. Clegg <i>Journal of Magnetism and Magnetic Materials</i> , 214 (2000) 3, 225-233
2610	Perforated tips for high-resolution in-plane magnetic force microscopy L. Folks, M. E. Best, P. M. Rice, B. D. Terris, D. Weller, and J. N. Chapman <i>Appl. Phys. Lett.</i> , 76 (2000) 909-911
1825	Carbon-nanotube probe equipped magnetic force microscope T. Arie, H. Nishijima, S. Akita and Y. Nakayama <i>J. Vac. Sci. Technol.</i> , B18 (2000) 1, 104-106
1207	Low temperature magnetic force microscopy with enhanced sensitivity based on piezoresistive detection A. Volodin, K. Temst, C. Van Haesendonck, and Y. Bruynseraede <i>Rev. Sci. Instrum.</i> , 71 (2000) 12, 4468-4473
642	Non-contact atomic force microscopy of an antiferromagnetic NiO(100) surface using a ferromagnetic tip H. Hosoi, M. Kimura, K. Hayakawa, K. Sueoka, K. Mukasa <i>Applied Physics A: Materials Science & Processing</i> , 72 (2001) 7, S23-S26
1835	Quantitative Analysis of the Magnetic Properties of a Carbon Nanotube Probe in Magnetic Force Microscopy T. Arie, N. Yoshida, S. Akita and Y. Nakayama <i>J. Phys. D: Appl. Phys.</i> , 34 (2001) L43-L45
2602	Magnetization reversal and coercivity of a single-domain Co/Pt dot measured with a calibrated magnetic force microscope tip J. Lohau, A. Carl, S. Kirsch, and E. F. Wassermann <i>Appl. Phys. Lett.</i> , 78 (2001) 14, 2020-2022
2603	Quantitative field measurements from magnetic force microscope tips and comparison with point and extended charge models S. McVitie, R. P. Ferrier, J. Scott, G. S. White, and A. Gallagher <i>J. Appl. Phys.</i> , 89 (2001) 7, 3656-3661
2598	Quantitative interpretation of magnetic force microscopy images from soft patterned elements J. M. Garcia et al. <i>Appl. Phys. Lett.</i> 79 (2001) 656
1148	Magnetic phase transitions studied by magnetic force microscopy Y.-A. Soh, G. Aeppli, N.D. Mathur, M.G. Blamire

	<i>Journal of Magnetism and Magnetic Materials</i> , 226 (2001) 857-859
2714	Quantitative interpretation of magnetic force microscopy images from soft patterned elements J. M. Garcia, A. Thiaville, J. Miltat, K. J. Kirk, J. N. Chapman, and F. Alouges <i>Appl. Phys. Lett.</i> , 79 (2001) 5, 656-658
2734	Computer Simulation of Magnetic Force Microscopy Images with a Static Model of Magnetization Distribution and Dipole-Dipole Interaction D. V. Ovchinnikov and A. A. Bukharaev <i>Tech. Phys.</i> , 46 (2001) 8, 1014
2705	Micromagnetic structure images taken using platinum coated tips O. Teschke <i>Appl. Phys. Lett.</i> , 79 (2001) 17, 2773-2775
2742	High resolution eddy current microscopy M. A. Lantz, S. P. Jarvis, and H. Tokumoto <i>Appl. Phys. Lett.</i> , 78 (2001) 3, 383-385
2752	Magnetic-field measurements of current-carrying devices by force-sensitive magnetic-force microscopy with potential correction Tony Alvarez, Sergei V. Kalinin, and Dawn A. Bonnell <i>Appl. Phys. Lett.</i> , 78 (2001) 7, 1005-1007
2648	Reconstruction of in-plane magnetization distributions from magnetic force microscope images T. Zhao, H. Fujiwara, G. J. Mankey, C. Hou, and M. Sun <i>J. Appl. Phys.</i> , 89 (2001) 11, 7230-7232
2663	Electrostatic charging artefacts in Lorentz electron tomography of MFM tip stray fields J. Scott, S. McVitie, R.P. Ferrier and A. Gallagher <i>Journal of Physics D: Applied Physics</i> , 34 (2001) 9, 1326-1332
2737	Current-modulating magnetic force microscope probe Frank Z. Wang, Na Helian, Warwick W Clegg, James F. C. Windmill, and David Jenkins <i>J. Appl. Phys.</i> , 89 (2001) 11, 6778-6780
2599	Calibrated magnetic force microscopy measurement of current-carrying lines R. Yongsunthon, J. McCoy, and E. D. Williams <i>J. Vac. Sci. Technol.</i> , A19 (2001) 4, 1763-1768
2569	Magnetization reversal and coercivity of magnetic-force microscopy tips A. Carl, J. Lohau, S. Kirsch, and E. F. Wassermann <i>J. Appl. Phys.</i> , 89 (2001) 11, 6098-6104
2635	Calibration of magnetic force microscopy using micron size straight current wires Congxiao Liu, Kingston Lin, Rich Holmes, Gary J. Mankey, Hideo Fujiwara, Huaming Jiang, and Hae Seok Cho <i>J. Appl. Phys.</i> , 91 (2002) 10, 8849-8851
1382	Self-sensing piezoresistive cantilever and its magnetic force microscopy applications Hiroshi Takahashi, Kazunori Ando and Yoshiharu Shirakawabe <i>Ultramicroscopy</i> , 91 (2002) 1-4, 63-72
2691	Magnetic force microscopy using focused ion beam sharpened tip with deposited antiferro-ferromagnetic multiple layers Zhiyong Liu, You Dan, Qiu Jinjun, and Yihong Wu <i>J. Appl. Phys.</i> , 91 (2002) 10, 8843-8845
2647	High resolution magnetic force microscopy using focused ion beam modified tips G. N. Phillips, M. H. Siekman, L. Abelmann, J. C. Lodder <i>Appl. Phys. Lett.</i> , 81 (2002) 5, 865-867
2731	Test of response linearity for magnetic force microscopy data R. Yongsunthon, E. D. Williams, J. McCoy, R. Pego, A. Stanishevsky, P. J. Rous

	<i>J. Appl. Phys.</i> , 92 (2002) 3, 1256-1261
2722	The extraction of features from magnetic force microscopy images using neural network techniques H. V. Jones and R. W. Chantrell <i>J. Appl. Phys.</i> , 91 (2002) 10, 8855-8857
2712	Quantitative analysis of transition curvature by magnetic force microscopy Feng Liu, Shaoping Li, Yan Liu, George Gray, and Allan Schultz <i>J. Appl. Phys.</i> , 91 (2002) 10, 6842-6844
2709	Orientation-sensitive magnetic force microscopy for future probe storage applications Dmitri Litvinov and Sakhrat Khizroev <i>Appl. Phys. Lett.</i> , 81 (2002) 10, 1878-1880
2428	Spin-polarized scanning tunneling microscopy with antiferromagnetic probe tips A. Kubetzka, M. Bode, O. Pietzsch, R. Wiesendanger <i>Phys. Rev. Lett.</i> , 88 (2002) 5, 57201
2198	Orientation-sensitive magnetic force microscopy for future probe storage applications Dmitri Litvinov and Sakhrat Khizroev <i>Appl. Phys. Lett.</i> , 81 (2002) 1878-1880
2639	Mapping electron flow using magnetic force microscopy R. Yongsunthon, A. Stanishevsky, E. D. Williams, and P. J. Rous <i>Appl. Phys. Lett.</i> , 82 (2003) 19, 3287-3289
2597	Magnetic force gradient mapping Tilman E. Schaffer, Manfred Radmacher, and Roger Proksch <i>J. Appl. Phys.</i> , 94 (2003) 10, 6525-6532
2645	High-resolution MFM: simulation of tip sharpening H. Saito, A. G. vanden Bos, L. Abelmann, J. C. Lodder <i>IEEE Trans Magn</i> , 39 (2003) 5, 3447-3449
2711	Point-dipole response from a magnetic force microscopy tip with a synthetic antiferromagnetic coating Yihong Wu, Yatao Shen, Zhiyong Liu, Kebin Li, and Jinjun Qiu <i>Appl. Phys. Lett.</i> , 82 (2003) 11, 1748-1750
2600	Real-space imaging of current distributions at the submicron scale using magnetic force microscopy: Inversion methodology P. J. Rous, R. Yongsunthon, A. Stanishevsky, and E. D. Williams <i>J. Appl. Phys.</i> , 95 (2004) 5, 2477-2486
2634	Calibration of magnetic force microscopy tips by using nanoscale current-carrying parallel wires Th. Kebe and A. Carl <i>J. Appl. Phys.</i> , 95 (2004) 3, 775-792



Site Search

Call us Toll-Free

In USA **866-SPMTIPS** (776-8477)
In Europe **8000-SPMTIPS** (776-8477)